RSC Advances

PAPER

View Article Online
View Journal | View Issue

Cite this: *RSC Adv.*, 2024, **14**, 34214

An innovative electrochemical sensor for brinzolamide detection in athletes' urine using a mercury–phen complex: a step forward in anti-doping†

Noha G. Abdel-Hafez, * Marwa F. B. Ali, Noha N. Atia and Samia M. El-Gizawy

Brinzolamide (BRZ) is an antiglaucoma drug also used by athletes for doping purposes; therefore, it is prohibited by the World Anti-Doping Agency. Consequently, the presence of BRZ or its metabolites in athletes' urine constitutes a violation of anti-doping rules. The current work presents a novel electrochemical method that assesses the effectiveness of mercury oxide nanoparticles (HgO-NPs) and a mercuric chloride–1,10-phenanthroline complex ($HgCl_2$–Phen complex) as sensors for BRZ analysis. A comparative analysis revealed that the synthesized $HgCl_2$–Phen complex exhibited superior sensitivity and efficiency in determining BRZ levels. The properties of the modifiers were extensively characterized using elemental analysis, X-ray diffraction (XRD), Fourier transform infrared (FT-IR) spectroscopy, and scanning electron microscopy (SEM). Furthermore, electrochemical characterization was conducted using square wave voltammetry (SWV), cyclic voltammetry (CV), and electrochemical impedance spectroscopy (EIS). The electrode showed a good response for SWV evaluations of BRZ in a concentration range of 0.1 to 6.0 μmol L^{-1}, with very low limits of detection (0.01 μmol L^{-1}) and quantitation (0.031 μmol L^{-1}). The method's applicability was validated by detecting BRZ in urine samples from healthy human volunteers and in pharmaceutical eye drops. Additionally, the practical effectiveness of the method was assessed using the blue applicability grade index (BAGI). The key advantages of this sensor include its simple manufacturing process, as well as its remarkable sensitivity and selectivity.

Received 12th September 2024
Accepted 22nd October 2024

DOI: 10.1039/d4ra06591c

rsc.li/rsc-advances

1. Introduction

Brinzolamide (BRZ) is an antiglaucoma drug, chemically known as (4*R*)-4-(ethylamino)-2-(3-methoxypropyl)-1,1-dioxo-3,4-dihydrothieno[3,2-e]thiazine-6-sulphonamide (Fig. S1A†).[1] BRZ is a highly selective, non-competitive, reversible, and efficient inhibitor of carbonic anhydrase II (CA-II) enzyme, which can reduce the intraocular pressure (IOP) by suppressing the production of aqueous humor in the eye.[2,3] Also, BRZ is used by athletes for doping purposes, as it has the potential to dilute urine samples and modify drug metabolism, thereby interfering with the urinalysis.[4] Accordingly, the World Anti-Doping Agency classified BRZ in the S5 list as a diuretic and masking agent.[5] BRZ preferentially distributes to erythrocytes, where it binds to the erythrocyte's CA-II enzyme; thus, single topical administration doesn't result in detectable amounts in either blood or urine. However, multiple administrations may result in plasma (and urine) levels near the minimum required performance level of 200 ng mL^{-1}.[6,7] Binding of the drug to the erythrocyte's CA-II enzyme increases its half-life, allowing it to remain in the body even after discontinuation of the drug.[6] Therefore, it's prohibited before and during competition.[8] Detection of BRZ or its metabolites in athletes' sample can be considered a violation of the anti-doping rules.[7]

Therefore, it is necessary to detect BRZ levels in athletes' samples to fight against doping in sports. Quantification of BRZ requires a highly sensitive, selective, reproducible, and cost-effective analytical method. Previous studies have reported the use of liquid chromatography,[9–11] thin layer chromatography,[12] and spectrophotometry[13,14] techniques. However, chromatographic methods involve the consumption of significant amounts of organic solvents and require multi-step sample preparation procedures. Additionally, the determination of BRZ in real samples requires measurement of lower concentrations than those reported in spectrophotometric methods. Therefore, the utilization of electrochemical techniques has been proposed as a viable alternative for the measurement and determination of organic compounds. Electrochemical methods are superior to other analytical methods due to their diverse applications, ultra-sensitivity, selectivity, as well as their cost-effectiveness and eco-friendliness.[15] Balashova *et al.*

Pharmaceutical Analytical Chemistry Department, Faculty of Pharmacy, Assiut University, Assiut, 71526, Egypt. E-mail: Noha_gamal@pharm.aun.edu.eg

† Electronic supplementary information (ESI) available. See DOI: https://doi.org/10.1039/d4ra06591c

reported a multisensory stripping voltammetry method to study the effect of some antiglaucoma drugs (including BRZ) on the tear fluid over time.[16] However, this method didn't establish a comprehensive study of the electrochemical behavior of BRZ, nor did it provide information on selectivity, sensitivity, detection limits, accuracy, and reliability. The previously reported method[16] was the only electrochemical method established for the analysis of BRZ till now. Therefore, the main purpose of this work is to address this gap and discuss our outcomes.

Mercury containing compounds have wide applications in electrochemistry due to their electrical conductance and versatility. For instance, mercuric oxide (HgO), which is a transition metal oxide, is classified as an n-type semiconductor and has been used as an electrochemical sensor for the analysis of several compounds.[17–19] HgO possesses a zinc blende structure,[17] and its bandgap is smaller than that of different metal oxides.[20] The bandgap has a significant effect on the electrical conductivity of substances: if a substance has a large bandgap, it is an insulator, whereas a substance with a smaller bandgap is a semiconductor.[21] Therefore, the electrical conductance of HgO is higher than that of other metal oxides, such as ZnO, CdO, and NiO.[20] These advantages indicate that HgO is a promising sensor in the field of electrochemistry. Additionally, mercuric chloride coordination polymers have been used for the electrochemical analysis of penicillin.[22]

The incorporation of metal complexes with carbon electrodes as electrochemical sensors is trending due to their wide applications and unique properties.[23–27] 1,10-Phenanthroline (1,10-Phen) (Fig. S1B†) is one of the most important complexing agents. The rigid structure of 1,10-Phen imposed by the central ring B gives it an extremely distinctive feature: the two nitrogen atoms are consistently maintained in juxtaposition.[28] Because of the aforementioned advantage, its complexes with metal ions can form rapidly. The complexation of 1,10-Phen with metal ions stabilizes them in a specific oxidation state and geometry, which may facilitate the transfer of electrons across the metal ions.[29] In the field of electrochemistry, 1,10-Phen has a great advantage as it doesn't undergo electrochemical reactions under normal conditions, and its oxidation to 1,10-Phen-5,6-dione requires a high potential (~2 V) *versus* Ag/AgCl,[30] or very strong chemical reactions; therefore, it can be considered an electrochemically inert compound.[31]

This work focuses, for the first time, on the study of the oxidation behavior of BRZ. HgO nanoparticles (HgO-NPs) and 1,10-Phen–$HgCl_2$ complex ($HgCl_2$–Phen complex) were synthetized for modification of a carbon paste electrode (CPE) for this purpose. Additionally, a clear discussion of the proposed oxidation mechanism of BRZ was included. This work aimed to establish a validated electrochemical method for determining BRZ concentration in athletes' urine samples to fight against doping in sports. Detection of BRZ in the urine of healthy human volunteers was also conducted after multiple dosing of BRZ to ensure the applicability of the current work. The produced $HgCl_2$–Phen complex was characterized with elemental analysis, powder X-ray diffraction (XRD), scanning electron microscopy (SEM) and Fourier transform infra-red (FT-IR). Finally, the blue applicability grade index (BAGI) was used to compare the proposed method with the previously reported methods in terms of practicality. The BAGI tool confirmed the very good performance of the current work. To the best of our knowledge, this is the first study which examine the electrochemical behavior of BRZ in urine samples and the first use of $HgCl_2$–Phen complex as an electrochemical sensor.

2. Experimental

2.1. Materials and reagents

Refer to ESI.†

2.2. Instrumentation

Refer to ESI.†

2.3. Synthesis of HgO-NPs

HgO-NPs were synthetized in accordance with a previous procedure with slight modifications.[32] Briefly, 14.54 mmol of mercuric(II) acetate ($Hg(OAc)_2$) was dissolved in nitric acid (1.38%). After that, a dropwise addition of 20 mL of NaOH (3.13 M) was added over the course of 1 hour. Then, 14.54 mmol of citric acid monohydrate was added dropwise over 2 hours. The formed yellow precipitate was washed with water and moved to a 100 mL autoclave, where it was treated for 2 hours at 150 °C. Finally, the precipitate was filtered, washed with distilled water several times, and dried for one day at 60 °C (Scheme 1A).

2.4. Synthesis of $HgCl_2$–Phen complex

1,10-Phen–metal complexes were synthesized using various methods as documented in the literature.[33–35] The $HgCl_2$–Phen complex was synthetized by a straightforward one-step modification of previously reported methods. The experimental procedure involved the dissolution of 216.5 mg (1 mmol) of the prepared HgO-NPs in 0.2 N HCl, followed by the addition of this solution to 198 mg (1 mmol) 1,10-Phen monohydrate in methanol under constant stirring for 30 min. Subsequently, a white compound ($HgCl_2$–Phen complex) was precipitated at room temperature (25 °C ± 4). Afterward, the precipitate was filtered off, washed several times with distilled water and methanol, and left to dry for 24 hours at 60 °C (yield: 90%) (Scheme 1B).

2.5. Fabrication of the working electrodes

In this study, a bare carbon paste electrode (BCPE) was fabricated by homogenously grinding 0.20 g ± 0.02 of graphite powder and subsequently mixing it with 25 μL of paraffin oil. The modified electrodes were created by blending 195 mg of graphite powder with 5 mg of the prepared HgO-NPs or 190 mg of graphite powder with 10 mg of the prepared $HgCl_2$–Phen complex for 10 minutes. Then, the mixture was thoroughly mixed with 25 μL of paraffin oil for an additional 10 minutes. The resultant paste was allowed to settle for 24 hours before being packed into a Teflon tube with a cavity diameter of 3 mm, reaching a depth of 1 cm. A copper wire was then inserted through the center of the electrode body to establish electrical connectivity with the paste.

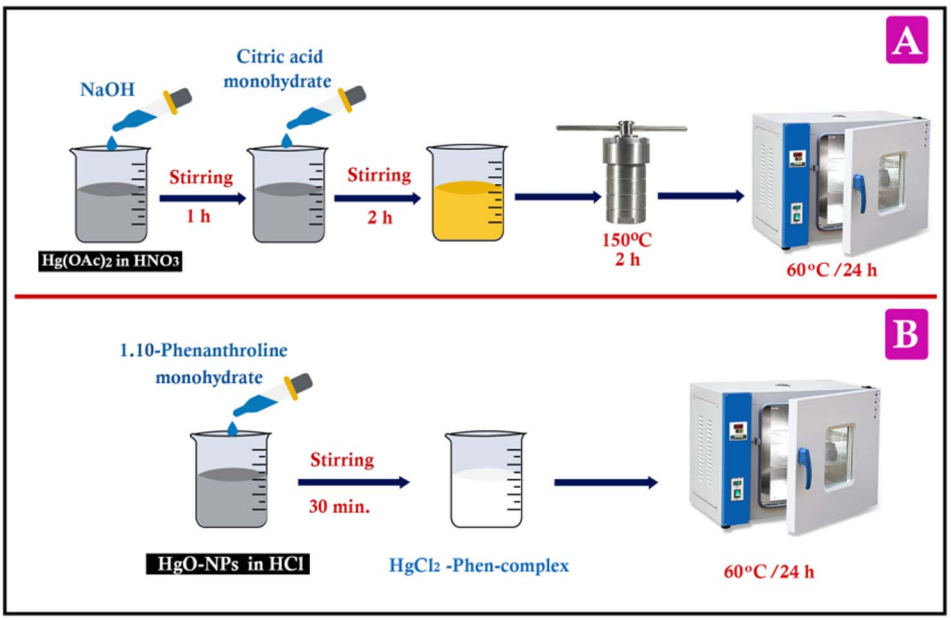

Scheme 1 Procedure of synthesis of (A) HgO-NPs, and (B) $HgCl_2$–Phen complex.

2.6. Preparation of the stock solutions

Refer to ESI.†

2.7. Electrochemical procedure

Square wave voltammetry (SWV) was utilized for the quantification of BRZ using the $HgCl_2$–Phen complex/CPE in Britton–Robinson (BR) buffer (pH of 7.5). The deposition potential (E_{dep}) was set at 0.3 V, and the deposition time (T_{dep}) was 180 s. SWV measurements were conducted with a frequency of 150 Hz, a step height of 10 mV, and a pulse height of 9 mV. Each scan was performed at a potential range from 0.3 V to 1.5 V at a scan rate of 0.10 V s^{-1}.

2.8. Electrochemical impedance spectroscopy (EIS)

Refer to ESI.†

2.9. Preparation of real samples

The study protocol was approved by the "Institutional Review Board" as well as the research ethics committee of the Faculty of Medicine at Assiut University, Assiut, Egypt (IRB approval number 04-2023-200631), for more details, refer to the ESI.†

3. Results and discussion

3.1. Characterization of the synthesized complex and fabricated electrodes

3.1.1. Elemental analysis and measurement of melting point. The elemental composition of the $HgCl_2$–Phen complex was investigated using CHN analysis, demonstrating congruence with the calculated values based on the chemical formula $HgCl_2(C_{12}H_8N_2)$ (Fig. 1A). Additionally, the confirmation of the complex formation was achieved through melting point determination, where the measured melting point of the starting material (1,10-Phen monohydrate) is 93–94 °C, while that of the prepared complex is >300 °C. These results are in good agreement with the reported results.[33]

3.1.2. X-ray diffraction (XRD) analysis. The $HgCl_2$–Phen complex was characterized using XRD analysis and compared with that of 1,10-Phen monohydrate, demonstrating that they are different (Fig. 1B). The as-prepared complex shows powder pattern with characteristic peaks at $2\theta = 7.3°$, 11.8°, 15.8°, 19°, 22°, 27.2°, 32°, 37°, and 43°. It's apparent that upon complexation, some peaks are shifted, some disappeared, and new set of 2θ values appeared. The appearance of new peaks and the disappearance of others suggests that the complexation with $HgCl_2$ has significantly altered the crystalline structure of 1,10-Phen monohydrate. The new peaks (*e.g.*, at 7.3, 11.3, 15.88, *etc.*) correspond to new sets of planes in the complexed material. These planes likely involve interactions between the phenanthroline, Hg^{2+} ions, and chloride ions. Lower 2θ peaks (*e.g.*, 7.3, 9.7). Likely correspond to planes with larger *d*-spacings, possibly involving atoms like Hg^{2+}, which, due to its large size and significant scattering factor, can contribute to reflections at lower angles. Higher 2θ peaks (*e.g.*, 28, 32.1, 43.7) typically correspond to planes with smaller *d*-spacings, which might be more influenced by the atomic layers closer together, such as those involving lighter atoms (C, N) or smaller interatomic distances within the phenanthroline rings or between Hg^{2+} and Cl^- ions. The peaks of the as-prepared complex are sharp indicating that the complex is well-ordered and stable.

3.1.3. FT-IR analysis of $HgCl_2$–Phen complex. FT-IR spectra of 1,10-phen monohydrate and $HgCl_2$–Phen complex are shown in Fig. 1C. The bands for 1,10-Phen are assigned and compared with the reported data. Upon complexation, the aromatic ring band, originally observed between 1644 and 1422 cm^{-1},

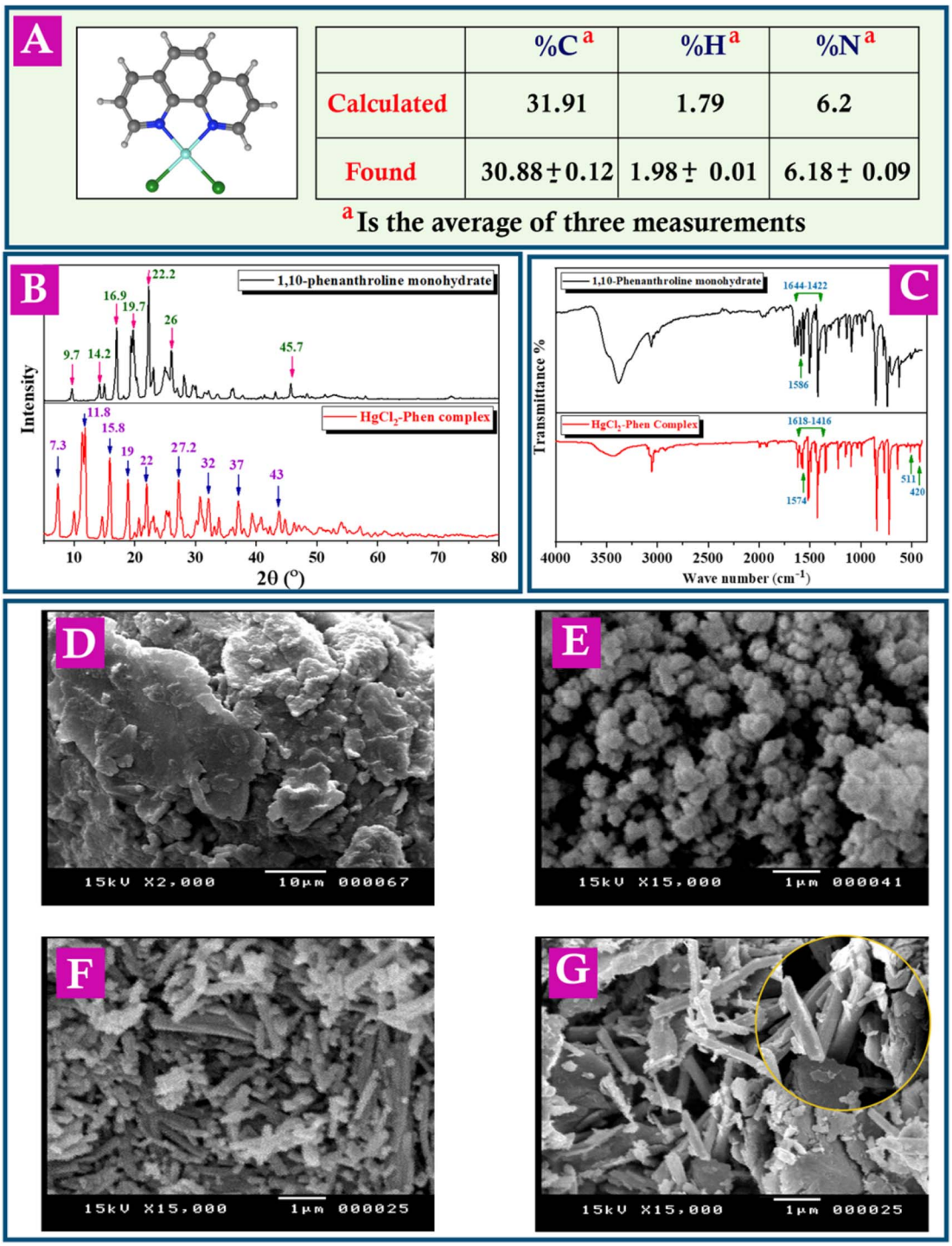

Fig. 1 (A) Elemental analysis of $HgCl_2$–Phen complex, (B and C) XRD patterns and FTIR spectra of 1,10-phen monohydrate and $HgCl_2$–Phen complex, respectively, and (D–G) SEM images of BCPE, HgO-NPs, $HgCl_2$–Phen complex, and $HgCl_2$–Phen complex/CPE, respectively.

underwent a downward shift to frequencies ranging from 1618 to 1416 cm^{-1}. The NH bonding vibration, initially recorded at 1586 cm^{-1} for the free ligand, experienced a frequency reduction to 1574 cm^{-1} due to complex formation. Additionally, the emergence of new bands at 511 and 420 cm^{-1} indicates the presence of Hg–N and Hg–Cl bonds, respectively.[36]

3.1.4. Scanning electron microscopy (SEM). The physical appearance and surface characteristics of BCPE, HgO-NPs, $HgCl_2$–Phen complex, and $HgCl_2$–Phen complex/CPE were evaluated using SEM to assess the surface morphology of the fabricated electrodes, as shown in Fig. 1. The SEM profile of BCPE (Fig. 1D) shows separated, unevenly shaped graphite

powder flakes. The SEM profile of HgO-NPs (Fig. 1E) shows separated sphere-like nanostructures.[37] SEM profile of $HgCl_2$–Phen complex (Fig. 1F) reveals the appearance of the micro-crystalline complex in the form of rods.[33] The SEM image of CPE modified with the $HgCl_2$–Phen complex is shown in Fig. 1G and shows distinguishable rods all over the electrode surface. It appears that modification increases the active surface area of the electrode by providing a more porous structure for the electrode surface, which enhances BRZ oxidation.

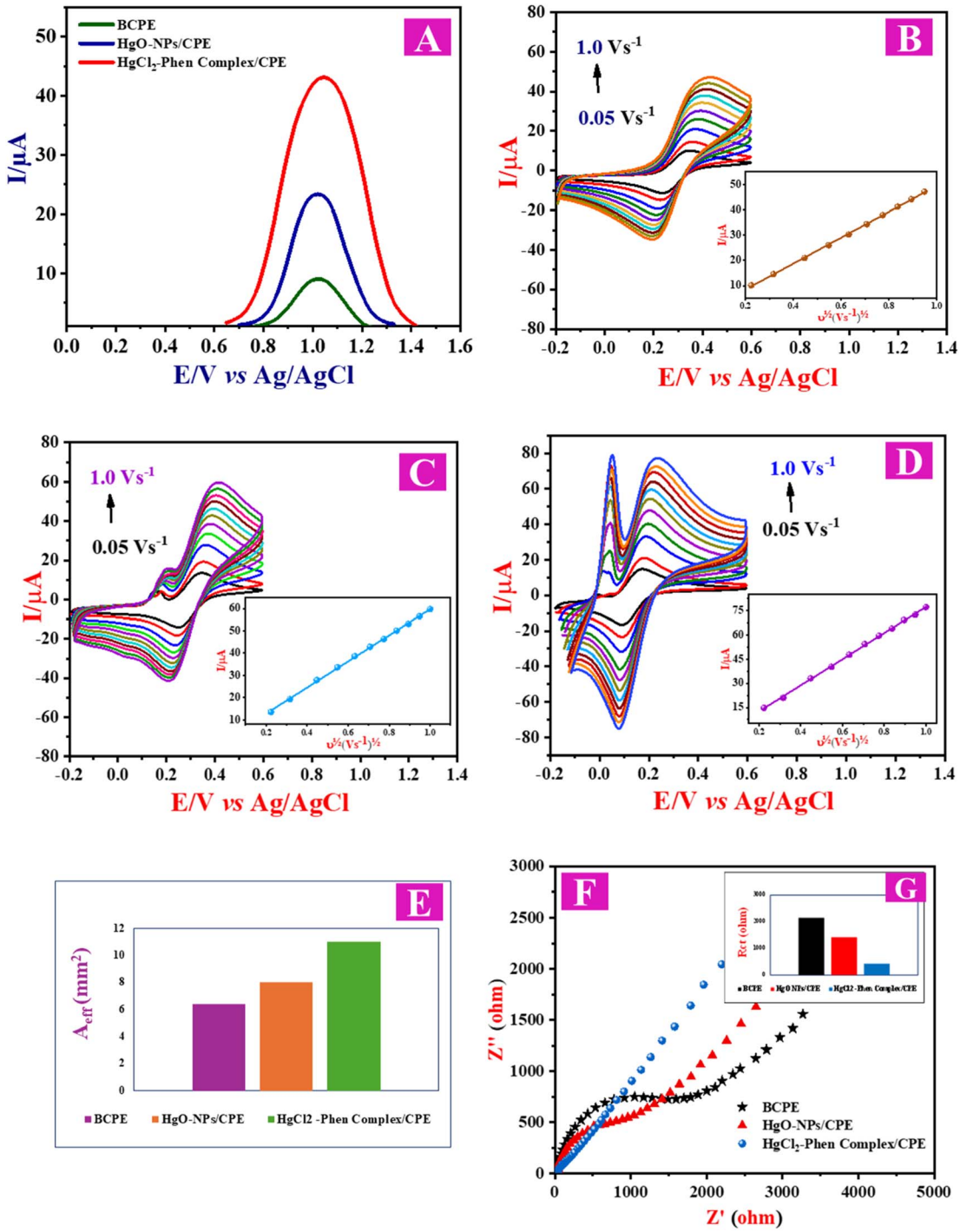

Fig. 2 (A) SWV of 4 µmol L^{-1} BRZ at BCPE, HgO-NPs/CPE and $HgCl_2$–Phen complex/CPE, CVs of $[Fe(CN)6]^{4-/3-}$ mixture (1.0 mmol L^{-1}) in KCl (0.5 mol L^{-1}) adjusted by HCl (1.0 mol L^{-1}) to pH 2.5 at (B) BCPE, (C) HgO-NPs/CPE, and (D) $HgCl_2$–Phen complex/CPE at different scan rates (0.05–1.0 V s^{-1}), (the anodic peak current relationship with the square root of scan rate was indicated as figure insets), (E) bar diagram of effective surface areas (mm^2) of different electrodes, (F) EIS Nyquist plots of BCPE, HgO-NPs/CPE and $HgCl_2$–Phen complex/CPE, and (G) bar diagram of R_{ct} values of different electrodes.

3.2. Electrochemical behavior of BRZ

The study of the electrochemical behavior of BRZ at modified and unmodified CPE was conducted using SWV. BCPE electrode showed a weak peak with a lower current response, as shown in Fig. 2A. However, when using HgO-NPs as an electrochemical sensor, an enhancement in the BRZ current was observed, and upon the complexation with 1,10-Phen, the intensity of the peak increased significantly (Fig. 2A). (This part will be discussed in detail in the section of Proposed oxidation mechanism.)

Other metal oxide nanoparticles, such as iron oxide and titanium oxide, were evaluated as electrochemical sensors; however, only minimal enhancements in the electrochemical behavior of BRZ were observed. Additionally, β-cyclodextrin was examined and displayed some improvement in the electrochemical response of BRZ, although this enhancement was not comparable to that achieved with the $HgCl_2$–Phen complex. Thus, this method is deemed the most efficient and sensitive for the application.

3.3. Surface area of bare and modified electrodes

A comparison between the effective surface areas (A_{eff}) of BCPE, HgO-NPs/CPE and $HgCl_2$–Phen complex/CPE was conducted using CVs in a solution of $[Fe(CN)_6]^{3-}/[Fe(CN)_6]^{4-}$ (1 : 1 mixture) at a concentration of 1.0 mmol L^{-1} dissolved in KCl (0.5 mol L^{-1}) and adjusted to pH 2.5 using HCl (1.0 mol L^{-1}), according to the Randles–Sevcik equation:[38]

$$I_p = 2.69 \times 10^5 n^{3/2} A_{eff} D^{1/2} \nu^{1/2} C \quad (1)$$

where: I_p (the anodic or cathodic peak current), A_{eff} (the effective electrode surface area), n (the number of electron transfer of potassium ferricyanide = 1), D (diffusion coefficient of potassium ferricyanide = 7.6×10^{-6} cm^2 s^{-1}), ν (the sweep rate), and C (the concentration of potassium ferricyanide = 1.0 mmol L^{-1}). By recording the CVs of each electrode at different sweep rates, the effective surface area of each electrode was calculated from the slope value of the relationship of I_p *vs.* $\nu^{1/2}$. When anodic peak current was used, the effective surface areas of BCPE, HgO-NPs/CPE, and $HgCl_2$–Phen complex/CPE were determined to be 6.91, 7.9, and 10.9 mm^2, respectively (Fig. 2B–E). The potential differences (ΔE_p) of CVs of ferricyanide/ferrocyanide on BCPE and $HgCl_2$–Phen complex/CPE were calculated at a sweep rate of 0.2 V s^{-1}. The broadened peak shape and significant difference in peak potential (ΔE_p = 151.24 mV) indicate the weakness of the electrochemical behavior of ferricyanide/ferrocyanide redox probe on BCPE. In contrast, for $HgCl_2$–Phen complex/CPE, ΔE_p was found to be 98.94 mV, and the peak current increased significantly, indicating the accelerated kinetics of electron transfer. The redox peaks of the $HgCl_2$–Phen complex/CPE at 0.0 V and 0.2 V (Fig. 2D) can be attributed to the oxidation of Hg(II), which confirms the presence of mercury ions in the manufactured sensor. The mercury ions are concentrated on the electrode surface so, upon transferring the electrode to the solution of 1.0 mmol L^{-1} $[Fe(CN)_6]^{3-}/[Fe(CN)_6]^{4-}$ (1 : 1 mixture) dissolved in KCl (0.5 mol L^{-1}) and adjusted to pH 2.5 using HCl (1.0 mol L^{-1}), the Hg^{2+} is electrochemically reduced to Hg^0 (eqn (2)), and then underwent oxidation to Hg^{2+} (eqn (3)).[39–42]

$$Hg^{2+} + 2e^- \rightarrow Hg^0 \quad (2)$$

$$Hg^0 \rightarrow Hg^{2+} + 2e^- \quad (3)$$

It is worth noting that this peak potential is sufficiently far from the potential range of BRZ oxidation in our study, that is in the range of (+0.3–1.5 V).

3.4. Electrochemical impedance spectroscopy (EIS)

The efficiency of electron transfer at different electrodes was displayed using the EIS in a solution of 1.0 mmol L^{-1} $[Fe(CN)_6]^{3-}/[Fe(CN)_6]^{4-}$ (1 : 1 mixture) dissolved in KCl (0.5 mol L^{-1}) and adjusted to pH 2.5 using HCl (1.0 mol L^{-1}). The impedance Nyquist plots of the BCPE, HgO-NPs/CPE and $HgCl_2$–Phen complex/CPE are displayed in Fig. 2F. The charge transfer resistances (R_{ct}) obtained at BCPE, HgO-NPs/CPE, and $HgCl_2$–Phen complex/CPE are illustrated in Table 1 and Fig. 2G, indicating that the CPE electrode modified with the $HgCl_2$–Phen complex had a lower resistance and a faster rate of electron transfer than the unmodified electrode. It is noteworthy to mention that the obtained values of R_{ct} are acceptable because transition metal structures are important semiconductor materials.

Additionally, the charge transfer rate (k_s) for the bare and modified electrodes was calculated from the EIS data using the following equation.[43]

$$K_s = RT/n^2F^2R_{ct}C \quad (4)$$

where C is the concentration of $[Fe(CN)_6]^{3-}/[Fe(CN)_6]^{4-}$ system, R = 8.314 J K^{-1} mol^{-1}, T is 25 °C, F = 96485 C mol^{-1}. The K_s values given in Table 1 confirm the enhancement of electron transfer reaction at the fabricated $HgCl_2$–Phen complex/CPE.

Furthermore, the electrochemical efficiency of the bare and modified electrodes was demonstrated by calculating the standard exchange current density (I_o) by using eqn (5).[44]

Table 1 Electrochemical results of 1 mM $[Fe(CN)_6]^{3-/4-}$ in 0.5 M KCl at different electrodes

	From CV		From EIS		
Electrode	ΔE_p (mV)	A_{eff} (mm^2)	R_{ct} (Ω)	K_s (cm s^{-1})	$I_o \times 10^{-5}$ (μA cm^{-1})
BCPE	151.24	6.91	2148	1.24×10^{-7}	1.19
HgO-NPs/CPE	127.1	7.9	1360	1.95×10^{-7}	1.88
$HgCl_2$–Phen complex/CPE	98.94	10.9	252	1.06×10^{-6}	10.18

$$I_o = RT/nFR_{ct} \quad (5)$$

The I_o value of the $HgCl_2$–Phen complex/CPE is 8.55 folds more than that of BCPE and 5.4 folds greater than that of HgO-NPs/CPE, which confirms the efficiency of the electrocatalytic activity of the $HgCl_2$–Phen complex/CPE.

3.5. Effect of sweep rate

CVs of BRZ were measured in BR buffer (pH 7.5) using the manufactured sensor ($HgCl_2$–Phen complex/CPE) at a range of sweeping rates (50–400 mV s^{-1}) to study the impact of the potential sweep rate (ν) on the drug's peak potential (E_p) and current (I_p) (Fig. 3A). As a result of increasing the potential sweep rate, the anodic oxidation peak currents (I_{pa}) increased, and the oxidation potential shifted to more positive values. A linear relationship between the logarithm of peak current (log I_p) and that of scan rate (log ν) is displayed in Fig. 3B, and the regression equation is as follows:

$$\text{Log } I_P\ (\mu A) = 1.832 + 0.611 \log \nu\ (\text{V s}^{-1})\ (r = 0.9989) \quad (6)$$

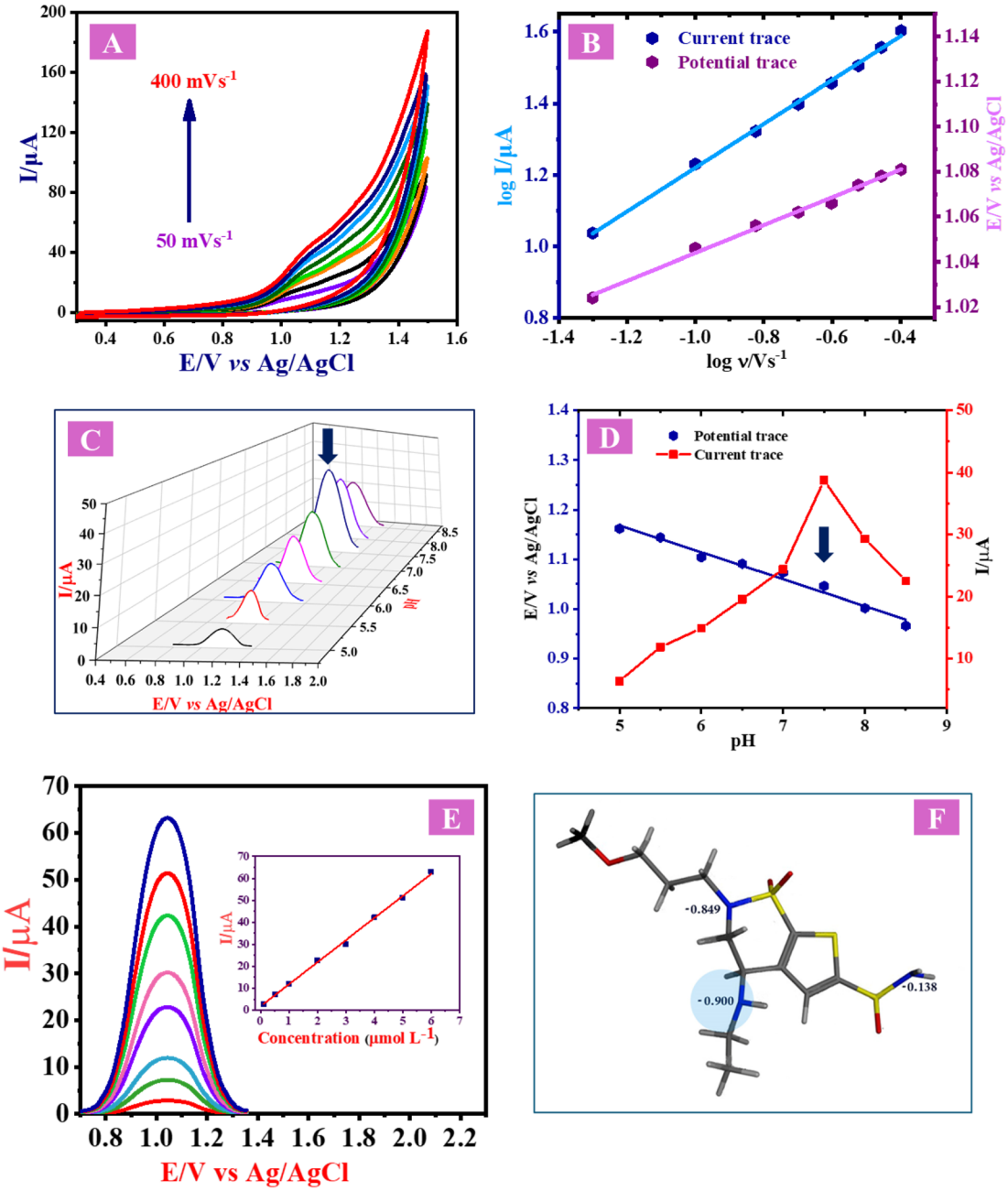

Fig. 3 (A) BRZ (2.5×10^{-5} mol L^{-1}) CVs at $HgCl_2$–Phen complex/CPE in BR buffer pH 7.5 obtained at different scan rates of 50–400 mV s^{-1}, (B) linear relationship of log I_p or E_p of BRZ on log ν. (C) SWV of 4 μmol L^{-1} BRZ at various pH values ranging from 5.0 to 8.5 at $HgCl_2$–Phen complex/CPE, (D) pH effect on 4 μmol L^{-1} BRZ peak potential and current at $HgCl_2$–Phen complex/CPE, (E) SWVs for BRZ different concentrations (0.1, 0.5, 1.0, 2.0, 3.0, 4.0, 5.0 and 6.0 μmol L^{-1}) in methanol together with the corresponding calibration curve (inset) at $HgCl_2$–Phen complex/CPE, and (F) 3D chemical structure of BRZ showing electron density of different nitrogen atoms using MOE software.

It was found that the slope value equals 0.611, which indicates that the electrooxidation process of BRZ is diffusion controlled. Fig. 3A confirms that the oxidation process of BRZ is irreversible due to the absence of a cathodic peak in the reverse CV sweep. E_p and log ν have a linear relationship, and the linear regression equation is as follows:

$$E_P\ (V) = 1.105 + 0.0617 \log \nu\ (V\ s^{-1})\ (r = 0.9970) \quad (7)$$

To estimate the number of electrons transferred during the oxidation of BRZ, the Laviron equation (eqn (8))[45] for an irreversible reaction can be used, where n is the measured number of electrons transferred, T is the absolute temperature (298 K), R is the universal gas constant (8.314 J mol^{-1} K^{-1}), and F is the Faraday's constant (96 480 C mol^{-1}).

$$\text{Slope} = 2.303RT/\alpha nF \quad (8)$$

The slope value is 0.0617, and considering the theoretical value of α is 0.5, the number of electrons (n) transferred equals 1.91–2.0 electrons. These results are in good agreement with previous studies done on similar medications.[46,47]

3.6. Effect of buffer pH on peak potential and peak current

One of the most important determining factors of the oxidation mechanism of a drug is the pH of the supporting electrolyte, as it affects various peak parameters such as peak current and potential. The assessment of the electrochemical oxidation mechanism was conducted over a pH range of 5.0 to 8.5, as shown in Fig. 3C. It is evident that BR buffer solution (pH 7.5) produced the maximum peak current. With increasing the pH values from 5.0 to 8.5, the peak potential shifted to the negative direction, which clearly indicates the involvement of protons in the oxidation process. A linear relationship between the pH range and peak potential shift is illustrated in Fig. 3D, with the following regression equation:

$$E_p\ (V) = 1.438 - 0.0541\text{pH}\ (n = 8 \text{ and } r = 0.9890) \quad (9)$$

From the previous regression equation, the slope of BRZ was 0.0541 V/pH, which is close to the theoretical value of 0.059 V/pH, indicating an equal contribution of protons and electrons in the oxidation process. These results are in good agreement with previous studies conducted on similar medications.[46,47]

3.7. Optimization of experimental and voltametric parameters

CPE components include graphite powder (the main component), paraffin oil (to induce cohesiveness) and the modifier ($HgCl_2$–Phen complex). These components should be optimized to obtain the best electrochemical behavior of BRZ on the modified electrode. The optimum amounts were found to be 0.2 g of graphite powder, 25 μL of paraffin oil, and 0.01 g of the $HgCl_2$–Phen complex, which constitutes 5% of the total amount of the paste.

Optimization of the deposition potential and time is essential, as these factors greatly affect the number of adsorbed drug molecules on the electrode surface. Consequently, the deposition potential was varied from 0 V to 0.5 V to obtain the largest anodic peak currents during SWV measurements at the modified electrode. The optimum deposition potential was found to be 0.3 V, as illustrated in Fig. S2A.† The deposition time was varied from 40 to 320 seconds, as illustrated in Fig. S2B,† and it was found that 180 seconds produced the highest current intensity.

Other voltametric parameters, such as step height, pulse height, and frequency, can also affect the intensity of peak current. After optimization, a step height of 10 mV, a pulse height of 9 mV, and a frequency of 150 Hz produced the optimum results.

3.8. Proposed oxidation mechanism

This research marks the first study that comprehensively examines the electrochemical behaviour of BRZ. Consequently, the investigation of its acid–base properties becomes pivotal in accurately elucidating its proposed oxidation mechanism on the manufactured electrode ($HgCl_2$–Phen complex/CPE). The pK_a values of BRZ (6.78 and 9.62) allow it to act as an acid or a base depending on the pH.[48] At pH 7.5, which is between the two pK_a values, BRZ is expected to exist as a zwitterionic species, with the sulfonamide group being deprotonated (carrying a negative charge) and the secondary amino group being protonated (carrying a positive charge).[49] On the other hand, the $HgCl_2$–Phen complex used as a modifier on the CPE is known to have a positively charged mercury(II) center (Hg^{2+}) coordinated by the neutral phenanthroline ligands. When BRZ interacts with the modified CPE at pH 7.5, the negatively charged sulfonamide group of BRZ can participate in an electrostatic interaction with the positively charged mercury(II) center of the $HgCl_2$–Phen complex. This electrostatic interaction between the oppositely charged species can lead to the adsorption or binding of BRZ onto the modified CPE surface.[50]

HgO-NPs enhance the oxidation behavior of BRZ due to the fact that nanoparticles have a large effective surface area, in addition to the electrical conductance of HgO as evidenced from the results of effective surface area and charge transfer resistance values, respectively. Upon complexation of Hg^{2+} ions with 1,10-Phen, the mercury is stabilized in a specific oxidation state and geometry as illustrated in Scheme 2. This stabilization may facilitate the transfer of electrons between BRZ and the mercury ions, thereby enhancing the oxidation process. These complexes are immobilized on the electrode surface and can create a more porous or roughened surface, which justifies the significant increase in the effective surface area of the electrode, thereby increasing the number of active sites available for the oxidation reaction.

It is worth noting that other types of interactions, such as π–π stacking interactions between the aromatic rings of BRZ and phenanthroline or hydrogen bonding interactions, may also contribute to the overall binding or adsorption process; however, the primary interaction at pH 7.5 is likely to be electrostatic in nature.

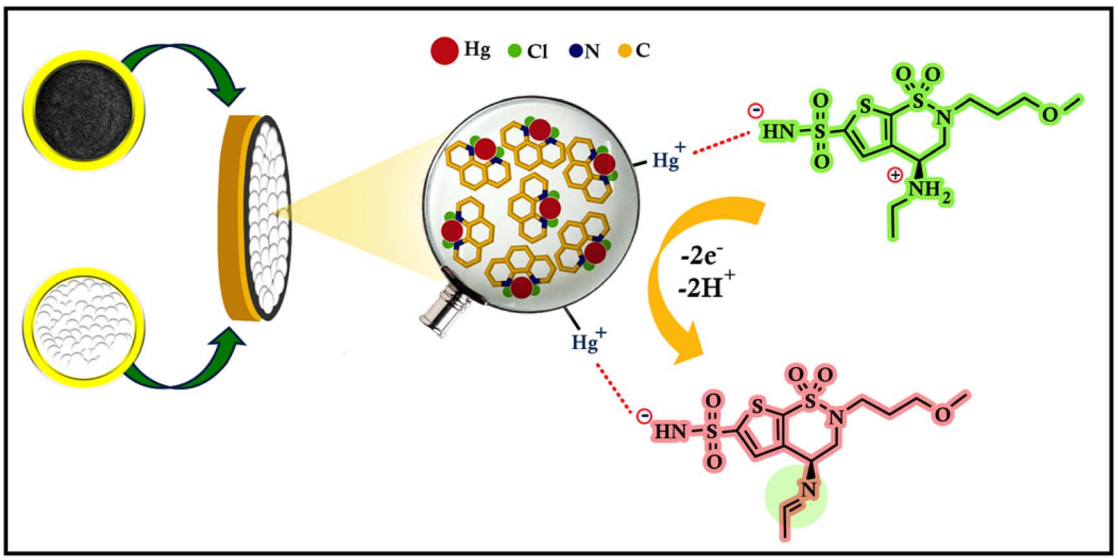

Scheme 2 Proposed oxidation mechanism of BRZ on $HgCl_2$–Phen complex/CPE.

The electrochemical oxidation of BRZ is suggested to occur at the secondary nitrogen atom (Fig. 3F). Utilizing the Molecular Operating Environment (MOE) program, the electron density of each nitrogen atom was assessed, revealing that the secondary nitrogen atom harbors the highest electron density (−0.900). This observation designates it as the most probable atom to undergo oxidation. Two electrons and two protons are lost during the oxidation of BRZ with subsequent formation of a double bond. These results are in good agreement with previous studies done on similar medications.[46,47]

3.9. Analytical investigations

The method's linearity was conducted using eight concentration levels of BRZ (Fig. 3E) at the $HgCl_2$–Phen complex/CPE using SWV in the range of 0.1–6 μmol L^{-1} according to the following regression equation:

$$I_P\ (\mu A) = 1.81 + 9.96C\ (\mu mol\ L^{-1})\ (r = 0.9971, n = 8) \quad (10)$$

The limits of detection (LOD) and quantitation (LOQ) are 0.01 and 0.031 μmol L^{-1}, respectively. LOD is expressed as $3.3\sigma/S$, and LOQ is expressed as $10\sigma/S$, where σ is the intercept's standard deviation and S is the slope. All these parameters are concluded in Table 2.

Table 2 Statistical data for BRZ determination using $HgCl_2$–Phen complex/CPE electrode in methanol

Parameter	Methanol
Linearity range (μmol L^{-1})	0.1–6
Correlation coefficient (r) ± SD[a]	0.9971 ± 0.00013
Determination coefficient (r^2) ± SD[a]	0.9943 ± 0.00029
Intercept (a) ± SD[a]	1.81 ± 0.031
Slope (b) ± SD[a]	9.96 ± 0.0195
LOD[b] (μmol L^{-1})	0.01
LOQ[b] (μmol L^{-1})	0.031

[a] Average of three replicates. [b] Detection (LOD) and quantification (LOQ) limits.

To prove that the method is accurate, three concentration levels (0.5, 2, and 5 μmol L^{-1}) of AZOPT® eye drops (10 mg BRZ per mL by Orchidia Pharmaceutical Industry, Al-Obour city, Egypt) were tested, with each concentration repeated six times. The percentage recoveries were calculated as represented in Table S1.†

These three concentrations were prepared from the BRZ stock solution and repeated six times in the same day and over 3 successive days to investigate the intra-day and inter-day precision of the method, respectively. The percentage recoveries varied from 99.43 to 100.72%, and RSD% didn't exceed 2.8%, ensuring that the method is truly precise, as shown in Table S1.†

The analytical method is considered robust when small modifications on the experimental parameters didn't lead to major changes in the drug recovery. To demonstrate the robustness of the suggested method, minor changes to some experimental parameters, such as the deposition potential, medium pH, and sweep rate, were applied, resulting in percentage recoveries ranging from 98.9 to 102.4%. These findings are represented in Table S2† and confirm the method's robustness.

3.10. Real samples application

3.10.1. Application to pharmaceutical eye drops. The method's applicability was demonstrated by analyzing BRZ in pharmaceutical eye drops. Table 3 illustrates the percentage recoveries of BRZ from AZOPT® eye drops (10 mg BRZ per mL, manufactured by Orchidia Pharmaceutical Industry, Al-Obour city, Egypt). The results showed acceptable recoveries (98.77–100.06%), indicating that there was no interference from pharmaceutical excipients. These results were statistically

Table 3 Assay of BRZ in eye drops and spiked human urine using $HgCl_2$–Phen complex/CPE electrode

Authentic drug	Sample	Claimed taken (μmol L^{-1})	Authentic added (μmol L^{-1})	Found concentration of added (μmol L^{-1})	% recovery ± SD[a]	RSD%
BRZ	AZOPT® eye drops (10 mg mL^{-1})	1	1	0.99	99.96 ± 0.95	0.95
			3	3.003	100.06 ± 0.70	0.70
			6	5.91	98.77 ± 1.12	1.14
	Human urine	1	0.5	0.49	98.53 ± 1.10	1.11
			1	1.02	102.67 ± 2.08	2.02
			3	3.02	100.59 ± 2.26	2.25
			6	5.95	99.03 ± 0.41	0.42

[a] Average of three replicates.

compared with those obtained from a reported method.[12] The calculated t and F values were 1.89 and 2.2, respectively (tabulated values for t and F were 2.23, 5.05, respectively), indicating the absence of a significant difference between the developed and reported method (Table S3†).

3.10.2. Application to spiked human urine samples. In spiked human urine samples, the obtained recoveries ranged from 98.53 to 102.67%, and RSD% values were acceptable. These results imply that the human urine matrix introduces no appreciable interference with the analysis of BRZ using the suggested method (Table 3).

3.10.3. Application to real human urine samples. The BRZ dose is 1 drop in each eye three times daily (~30 μL of 1% solution).[51] By following this regime, BRZ primarily binds to CA-II enzyme in red blood cells, then accumulation of the drug continued for 8 days until reaching a concentration of 20–25 μM, which is the concentration of CA-II in the blood. BRZ cannot be detected in the initial eight days since CA-II sites are being saturated. At a steady state, renal excretion of BRZ increases, making it detectable in urine.[52] In the present study, urine samples were analyzed under the specified conditions in Section 2.7. BRZ remained undetectable in urine samples of healthy volunteers during the first nine days. However, by the tenth day, BRZ was identified in only three samples, and by the eleventh day, it was detected in all collected samples. These results demonstrate the effectiveness of the current method in detecting BRZ, particularly in the context of its illegal use by athletes for doping.

3.11. Selectivity

A fundamental attribute of the modified electrode lies in its selectivity for analyzing the targeted drug in the presence of anticipated interferences. AZOPT® eye drops (10 mg BRZ per mL by Orchidia Pharmaceutical Industry, Al-Obour city, Egypt) contains BRZ along with various excipients such as benzalkonium chloride, sodium chloride, mannitol, and additional additives.[53] The results confirmed that the drug's oxidation wasn't affected in the presence of 50-fold mannitol and 75-fold of each of benzalkonium chloride or sodium chloride (the change in signal is ≤±5.0%). To further confirm the selectivity of the proposed method, spiking of urine samples with 1, 3, and 5 μmol L^{-1} BRZ and different ratios of interfering species, such as uric and ascorbic acid was conducted. The results confirmed that the drug's oxidation wasn't affected in presence of 50-fold of each of uric and ascorbic acids (the change in signal is ≤±5.0%). Additionally, the oxidation of uric acid and ascorbic acid occurs at low potentials (0.25 and 0.11 V, respectively), which are far from the peak potential of BRZ in our methodology, which is about 1.04 V. The obtained findings confirm the high selectivity of this work.

3.12. Comparison of the current work with the reported methods and blueness evaluation

The proposed SWV method was compared with reported methods for the analysis of BRZ in biological fluids, regarding the technique used, limit of detection, linearity range and matrix (Table 4). Additionally, a comparison between these methods in terms of their applicability was accomplished using the BAGI tool.[56] The BAGI method is an excellent attribute that allows the comparison of different analytical methods in terms of practicality and performance. The BAGI assessment uses four distinct scores, each assigned to a different color hue. The scores are 10, 7.5, 5.0, and 2.5 points, representing dark blue, blue, light blue, and white, respectively. Dark blue indicates high compliance, and as the degree of the color blueness decreases, the degree of compliance decreases. The central number of the pictogram is between 25 to 100, with 25 indicating poor performance and 100 indicating excellent performance. A method is deemed practical if it scores at least 60 points.

It is worth noting that the proposed method has good applicability, simplicity, novelty, sensitivity and selectivity. Methods based on HPLC-MS/MS, despite of their sensitivity, are very expensive, complicated, and require high experience and multi-step preparation procedures. Table S4† shows the 10 factors utilized in evaluation of the practicality of the proposed method using the BAGI method.

3.13. Future perspectives and limitations of the current work

Future studies could focus on validating the electrochemical sensor in real-world sports settings to ensure reliability and accuracy in diverse conditions, such as varying pH levels and

Table 4 Comparison of the proposed method with the previously reported methods

Technique	Linearity	LOQ	Matrix	BAGI	Ref.
LC-QTOF-MS/MS	0.500–20.00 μg mL^{-1}	—	Dried blood spots		9
LC-MS/MS	0.05–5.00 μg mL^{-1}	50 ng mL^{-1}	Rabbit aqueous humor		10
UHPLC-MS/MS	(7.00×10^{-4} to 0.50 μg mL^{-1} in urine) and (6.00×10^{-4} to 0.01 μg mg^{-1} in hair)	0.07 ng mL^{-1} in urine and 0.06 ng mg^{-1} in hair	Human urine and hair		11
LC-UV	0.10–1.00 μg mL^{-1}	100.0 ng mL^{-1}	Rabbit aqueous humor		54
HPLC-DAD	0.001–1.00 μg mL^{-1}	0.41 ng mL^{-1}	Human urine	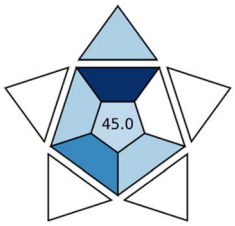	55
Voltammetry	0.04–2.30 μg mL^{-1}	11.88 ng mL^{-1}	Bulk, ophthalmic formulation, and human urine		This work

ionic strengths in urine samples. Additionally, the sensor's applicability for detecting other prohibited substances or their metabolites could be investigated to expand its utility in doping control. Also, further research could explore modifications to the sensor design, such as integrating nanomaterials or conducting polymer coatings, in order to enhance sensitivity and selectivity. It will be interesting to develop portable devices for on-site testing which could facilitate immediate doping control in athletic events, making the process more efficient. Finally, engaging with regulatory bodies to ensure that the proposed methods align with international standards for doping control could enhance their acceptance in professional sports.

The major limitation of this method is the environmental implications of using mercury-based materials in sensor

development. This impact should be carefully considered, particularly regarding disposal and potential toxicity.

4. Conclusion

The current study presents a novel blue electrochemical method for detecting BRZ; an antiglaucoma drug; which is banned by the World Anti-Doping Agency due to its misuse by athletes. By comparing the performance of HgO-NPs and the $HgCl_2$–Phen complex as electrochemical sensors, the $HgCl_2$–Phen complex was found to be more sensitive and efficient for BRZ detection. Various characterization techniques were used to confirm the formation of the modifier as elemental analysis, XRD, FT-IR, and SEM. The electrocatalysis of the drug was enhanced by the very good conductivity of the manufactured electrode and its high effective surface area. Low BRZ detection limit (10 nmol L^{-1}) indicates the high sensitivity of the proposed method which ensures its applicability for analysis of BRZ in various matrices. The current work could detect BRZ in the urine of healthy human volunteers which confirms its usefulness in fighting against doping in sports.

Ethical statement

The study protocol was approved in 21/12/2023 by the "Institutional Review Board" as well as the research ethics committee of the Faculty of Medicine in Assiut University, Assiut, Egypt (IRB approval number 04-2023-200631), applicable to human and animal studies, urine samples were collected from human volunteers. Prior to participation, all sampled subjects were duly informed, and their consent was obtained.

Data availability

The data supporting this article have been included as part of the ESI.†

Author contributions

Noha G. Abdel-Hafez: conceptualization; investigation; data curation; methodology; resources; validation; writing original draft. Marwa F. B. Ali: conceptualization; methodology; data curation; formal analysis; supervision; visualization; writing-review and editing. Noha N. Atia: conceptualization; project administration; writing-review and editing; supervision. Samia M. El-Gizawy: conceptualization; project administration; writing-review and editing; supervision.

Conflicts of interest

There are no conflicts to declare.

Acknowledgements

This research did not receive any specific grant from funding agencies in the public, commercial, or not-for-profit sectors.

References

1 National Center for Biotechnology Information, *PubChem Compound Summary for CID 68844, Brinzolamide*, 2024, Retrieved October 2, 2024, from: **https://pubchem.ncbi.nlm.nih.gov/compound/Brinzolamide**.

2 M. Iester, Brinzolamide ophthalmic suspension: a review of its pharmacology and use in the treatment of open angle glaucoma and ocular hypertension, *Clin. Ophthalmol.*, 2008, **2**(3), 517–523, DOI: **10.2147/opth.s3182**.

3 R. S. Cvetkovic and C. M. Perry, Brinzolamide: a review of its use in the management of primary open-angle glaucoma and ocular hypertension, *Drugs Aging*, 2003, **20**, 919–947, DOI: **10.2165/00002512-200320120-00008**.

4 A. B. Cadwallader, X. De La Torre, A. Tieri and F. Botrè, The abuse of diuretics as performance-enhancing drugs and masking agents in sport doping: pharmacology, toxicology and analysis, *Br. J. Pharmacol.*, 2010, **161**(1), 1–16, DOI: **10.1111/j.1476-5381.2010.00789.x**.

5 B. van der Sloot, M. Paun, R. Leenes, B. van der Sloot, M. Paun and R. Leenes, The World Anti-Doping Agency and Its Rules, *Athletes' Human Rights and the Fight Against Doping: A Study of the European Legal Framework*. 2020, pp. 5–129.

6 R. S. Kadam, G. Jadhav, M. Ogidigben and U. B. Kompella, Ocular pharmacokinetics of dorzolamide and brinzolamide after single and multiple topical dosing: implications for effects on ocular blood flow, *Drug Metab. Dispos.*, 2011, **39**(9), 1529–1537, DOI: **10.1124/dmd.111.040055**.

7 A. Pokrywka, M. Skrzypiec-Spring, J. Krzywański, M. Rynkowski, M. Saugy and R. Faiss, Cases reports: Unintended anti-doping rule violation after dorzolamide use several months prior to a doping control, *Drug Test. Anal.*, 2021, **13**(10), 1803–1806, DOI: **10.1002/dta.3156**.

8 A. B. Cadwallader, X. De La Torre, A. Tieri and F. Botrè, The abuse of diuretics as performance-enhancing drugs and masking agents in sport doping: pharmacology, toxicology and analysis, *Br. J. Pharmacol.*, 2010, **161**(1), 1–16.

9 A. Foivas, A. Malenović, N. Kostić, M. Božić, M. Knežević and Y. L. Loukas, Quantitation of brinzolamide in dried blood spots by a novel LC-QTOF-MS/MS method, *J. Pharm. Biomed. Anal.*, 2016, **119**, 84–90, DOI: **10.1016/j.jpba.2015.11.043**.

10 S. T. Hassib, E. F. Elkady and R. M. Sayed, Simultaneous determination of timolol maleate in combination with some other anti-glaucoma drugs in rabbit aqueous humor by high performance liquid chromatography–tandem mass spectroscopy, *J. Chromatogr. B*, 2016, **1022**, 109–117, DOI: **10.1016/j.jchromb.2016.04.012**.

11 A. F. Lo Faro, A. Tini, M. Gottardi, F. Pirani, A. Sirignano, R. Giorgetti, *et al.*, Development and validation of a fast ultra-high-performance liquid chromatography tandem mass spectrometry method for determining carbonic anhydrase inhibitors and their metabolites in urine and hair, *Drug Test. Anal.*, 2021, **13**(8), 1552–1560, DOI: **10.1002/dta.3055**.

12 M. S. Eissa, I. M. Nour, M. R. Elghobashy and M. A. Shehata, Validated TLC-densitometry method for simultaneous determination of brinzolamide and timolol in their ophthalmic preparation, *Anal. Chem. Lett.*, 2017, **7**(6), 805–812, DOI: 10.1080/22297928.2017.1395294.

13 S. Tambe, S. S. Das, K. Shahane, S. K. Singh, J. Ruokolainen, P. Amin, *et al.*, First-order derivative spectrophotometric method for simultaneous determination of brinzolamide and timolol maleate in ophthalmic formulation, *Green Anal. Chem.*, 2024, **8**, 100098, DOI: 10.1016/j.greeac.2024.100098.

14 V. Shah and H. Raj, Development and validation of derivative spectroscopic method for simultaneous estimation of cefixime trihydrate and azithromycin dihydrate in combined dosage form, *Int. J. Pharm. Sci. Res.*, 2012, **3**(6), 1753.

15 A. J. Bard, L. R. Faulkner and H. S. White, *Electrochemical Methods: Fundamentals and Applications*, John Wiley & Sons, 2022.

16 L. Balashova, N. Bakunina, V. Namiot, I. Kolesnichenko, Y. D. Kuznetsova, A. Balashov, *et al.*, A Multisensory Stripping Voltammetry Method for Analysis of Anti-Glaucoma Drugs, *Biophysics*, 2022, **67**(4), 660–666, DOI: 10.1134/S0006350922040030.

17 Z. Hanafi and F. Ismail, Colour problem of mercuric oxide photoconductivity and electrical conductivity of mercuric oxide, *Z. Phys. Chem.*, 1988, **158**(1), 81–86, DOI: 10.1524/zpch.1988.158.Part_1.081.

18 S. Y. Alfaifi, M. M. Hussain, A. M. Asiri and M. M. Rahman, Glassy Carbon Electrodes Decorated with HgO/CNT Nanocomposite and Modified with a Conducting Polymer Matrix for Enzyme-Free Ascorbic Acid Detection, *ChemistrySelect*, 2022, **7**(14), e202200086, DOI: 10.1002/slct.202200086.

19 J.-Y. Choi, K. Seo, S.-R. Cho, J.-R. Oh, S.-H. Kahng and J. Park, Screen-printed anodic stripping voltammetric sensor containing HgO for heavy metal analysis, *Anal. Chim. Acta*, 2001, **443**(2), 241–247, DOI: 10.1016/S0003-2670(01)01219-3.

20 J. Portier, H. Hilal, I. Saadeddin, S. Hwang, M. Subramanian and G. Campet, Thermodynamic correlations and band gap calculations in metal oxides, *Prog. Solid State Chem.*, 2004, **32**(3–4), 207–217, DOI: 10.1016/j.progsolidstchem.2005.05.001.

21 Y. N. Patil, M. B. Megalamani and S. T. Nandibewoor, A novel nanozyme doped ZnO/r-GO-based sensor for highly sensitive electrochemical determination of muscle-relaxant drug: cyclobenzaprine HCl, *Microchim. Acta*, 2024, **191**(6), 336, DOI: 10.1007/s00604-024-06418-w.

22 Y. Q. Xue, Y. Bi and J. Chen, Halide-directed Assembly of Mercury (II) Coordination Polymers for Electrochemical Biosensing Toward Penicillin, *Z. Anorg. Allg. Chem.*, 2020, **646**(5), 296–300, DOI: 10.1002/zaac.201900322.

23 S. Narouie, M. Shahbakhsh, Z. Hashemzaei, A. Nouri, H. Saravani and M. Noroozifar, Modified graphite paste electrode with strontium phen-dione complex for simultaneous determination of a ternary mixture of 4-aminophenol, uric Acid and tryptophan (Part I), *Int. J. Electrochem. Sci.*, 2017, **12**(11), 10911–10932, DOI: 10.20964/2017.11.09.

24 X. Liu, X. Li, Y. Xiong, Q. Huang, X. Li, Y. Dong, *et al.*, A glassy carbon electrode modified with the nickel (II)-bis (1,10-phenanthroline) complex and multi-walled carbon nanotubes, and its use as a sensor for ascorbic acid, *Microchim. Acta*, 2013, **180**, 1309–1316, DOI: 10.1007/s00604-013-1058-8.

25 U. P. Azad, S. Turllapati, P. K. Rastogi and V. Ganesan, Tris (1,10-phenanthroline) iron (II)-bentonite film as efficient electrochemical sensing platform for nitrite determination, *Electrochim. Acta*, 2014, **127**, 193–199, DOI: 10.1016/j.electacta.2014.02.012.

26 A. Kassa, A. Abebe and M. Amare, Synthesis, characterization, and electro polymerization of a novel Cu (II) complex based on 1,10-phenanthroline for electrochemical determination of amoxicillin in pharmaceutical tablet formulations, *Electrochim. Acta*, 2021, **384**, 138402, DOI: 10.1016/j.electacta.2021.138402.

27 İ. Koçak and F. Pekdemir, Non-Enzymatic Electrochemical Detection of Hydrogen Peroxide and Glucose through Using Copper (II) and Platinum (II) Complexes with Tridentate Ligand–Platinum Nanoparticles–Graphene Oxide Composite, *J. Electrochem. Soc.*, 2023, **170**(6), 066501, DOI: 10.1149/1945-7111/acd7a9.

28 W. W. Brandt, F. P. Dwyer and E. D. Gyarfas, Chelate complexes of 1,10-phenanthroline and related compounds, *Chem. Rev.*, 1954, **54**(6), 959–1017, DOI: 10.1021/cr60172a003.

29 A. Bencini and V. Lippolis, 1,10-Phenanthroline: A versatile building block for the construction of ligands for various purposes, *Coord. Chem. Rev.*, 2010, **254**(17–18), 2096–2180, DOI: 10.1016/j.ccr.2010.04.008.

30 G. Prakasam and A. Senthil Kumar, Electrochemical Behavior of the 1,10-Phenanthroline Ligand on a Multiwalled Carbon Nanotube Surface and Its Relevant Electrochemistry for Selective Recognition of Copper Ion and Hydrogen Peroxide Sensing, *Langmuir*, 2014, **30**, 10513–10521.

31 F. Calderazzo, F. Marchetti, G. Pampaloni and V. Passarelli, Co-ordination properties of 1,10-phenanthroline-5, 6-dione towards group 4 and 5 metals in low and high oxidation states, *J. Chem. Soc., Dalton Trans.*, 1999, (24), 4389–4396.

32 E. A. Abdelrahman and R. Hegazey, Facile synthesis of HgO nanoparticles using hydrothermal method for efficient photocatalytic degradation of crystal violet dye under UV and sunlight irradiation, *J. Inorg. Organomet. Polym. Mater.*, 2019, **29**, 346–358, DOI: 10.1007/s10904-018-1005-6.

33 M. Ranjbar, E. Malakooti and S. Sheshmani, Synthesis and Characterization of Mercury (II) Complexes Containing 2, 9-Dimethyl-1,10-phenanthroline by Sonochemical Method, *J. Chem.*, 2013, **2013**(1), 560983, DOI: 10.1155/2013/560983.

34 W. H. Mahmoud, G. G. Mohamed and M. M. El-Dessouky, Synthesis, characterization and in vitro biological activity of mixed transition metal complexes of lornoxicam with 1,10-phenanthroline, *Int. J. Electrochem. Sci.*, 2014, **9**(3), 1415–1438, DOI: 10.1016/S1452-3981(23)07804-5.

35 E. Ismail, D. Sabry, H. Mahdy and M. Khalil, Synthesis and Characterization of some Ternary Metal Complexes of Curcumin with 1,10-phenanthroline and their Anticancer Applications, *J. Sci. Res.*, 2014, **6**(3), 509–519, DOI: 10.3329/jsr.v6i3.18750.

36 K. Nakamoto, *Infrared and Raman Spectra of Inorganic and Coordination Compounds, Part B: Applications in Coordination, Organometallic, and Bioinorganic Chemistry*, John Wiley & Sons, 2009.

37 A. Mohadesi, M. Ranjbar and S. Hosseinpour-Mashkani, Solvent-free synthesis of mercury oxide nanoparticles by a simple thermal decomposition method, *Superlattices Microstruct.*, 2014, **66**, 48–53, DOI: 10.1016/j.spmi.2013.11.017.

38 P. Zanello, C. Nervi and F. F. De Biani, Inorganic electrochemistry: theory, practice and application, Royal Society of Chemistry, 2019.

39 D. Han, Y.-R. Kim, J.-W. Oh, T. H. Kim, R. K. Mahajan, J. S. Kim, *et al.*, A regenerative electrochemical sensor based on oligonucleotide for the selective determination of mercury (II), *Analyst*, 2009, **134**(9), 1857–1862, DOI: 10.1039/B908457F.

40 N. Wang, M. Lin, H. Dai and H. Ma, Functionalized gold nanoparticles/reduced graphene oxide nanocomposites for ultrasensitive electrochemical sensing of mercury ions based on thymine–mercury–thymine structure, *Biosens. Bioelectron.*, 2016, **79**, 320–326, DOI: 10.1016/j.bios.2015.12.056.

41 M. Amiri, H. Salehniya and A. Habibi-Yangjeh, Graphitic carbon nitride/chitosan composite for adsorption and electrochemical determination of mercury in real samples, *Ind. Eng. Chem. Res.*, 2016, **55**(29), 8114–8122, DOI: 10.1021/acs.iecr.6b01699.

42 A. M. Ashrafi, Z. Koudelkova, E. Sedlackova, L. Richtera and V. Adam, Electrochemical sensors and biosensors for determination of mercury ions, *J. Electrochem. Soc.*, 2018, **165**(16), B824, DOI: 10.1149/2.0381816jes.

43 P. Veerakumar, A. Sangili, S.-M. Chen, V. Vinothkumar, S. Balu, S.-T. Hung, *et al.*, Zinc and sulfur codoped iron oxide nanocubes anchored on carbon nanotubes for the detection of antitubercular drug isoniazid, *ACS Appl. Nano Mater.*, 2021, **4**(5), 4562–4575, DOI: 10.1021/acsanm.1c00172.

44 H. Ibrahim and Y. Temerk, Surface decoration of functionalized carbon black nanoparticles with nanosized gold particles for electrochemical sensing of diuretic spironolactone in patient plasma, *Microchem. J.*, 2022, **178**, 107425, DOI: 10.1016/j.microc.2022.107425.

45 E. Laviron, General expression of the linear potential sweep voltammogram in the case of diffusionless electrochemical systems, *J. Electroanal. Chem. Interfacial Electrochem.*, 1979, **101**(1), 19–28, DOI: 10.1016/S0022-0728(79)80075-3.

46 H. A. Hendawy, H. M. Elwy and A. M. Fekry, Electrochemical and chemometric determination of dorzolamide and timolol in eye drops using modified multiwall carbon nanotube electrode, *Int. J. Pharm. Pharm. Sci.*, 2017, **9**(9), 43–50.

47 V. Shakibaian and M. H. Parvin, Determination of acetazolamide by graphene paste electrode, *J. Electroanal. Chem.*, 2012, **683**, 119–124, DOI: 10.1016/j.jelechem.2012.07.042.

48 V. Naageshwaran, V.-P. Ranta, G. Gum, S. Bhoopathy, A. Urtti and E. M. Del Amo, Comprehensive ocular and systemic pharmacokinetics of brinzolamide in rabbits after intracameral, topical, and intravenous administration, *J. Pharm. Sci.*, 2021, **110**(1), 529–535, DOI: 10.1016/j.xphs.2020.09.051.

49 K. Mazák and B. Noszál, Physicochemical properties of zwitterionic drugs in therapy, *ChemMedChem*, 2020, **15**(13), 1102–1110, DOI: 10.1002/cmdc.202000164.

50 Z. Adamczyk and P. Warszyński, Role of electrostatic interactions in particle adsorption, *Adv. Colloid Interface Sci.*, 1996, **63**, 41–149, DOI: 10.1016/0001-8686(95)00281-2.

51 R. S. Cvetkovic and C. M. Perry, Brinzolamide: a review of its use in the management of primary open-angle glaucoma and ocular hypertension, *Drugs Aging*, 2003, **20**, 919–947, DOI: 10.2165/00002512-200320120-00008.

52 L. DeSantis, Preclinical overview of brinzolamide, *Surv. Ophthalmol.*, 2000, **44**, S119–S29, DOI: 10.1016/S0039-6257(99)00108-3.

53 https://www.medsafe.govt.nz/profs/datasheet/a/Azopteyedrop.pdf.

54 M. A. Wahab Mubarak, M. A.-A. Mohammad, R. I. El-Bagary, E. Elkady and N. F. Abo-Talib, A Simple Validated LC-UV Method for the Simultaneous Determination of Brimonidine and Brinzolamide in the Presence of Brinzolamide's Degradation Product (Major Metabolite) in Rabbit Aqueous Humor, *J. Chromatogr. Sci.*, 2024, bmae040, DOI: 10.1093/chromsci/bmae040.

55 M. Liu, B. Lv, H. Jiang, P. Yuan, H. Zhu and B. Gao, Determination of diuretics in human urine using HPLC coupled with magnetic solid-phase extraction based on a metal–organic framework, *Biomed. Chromatogr.*, 2020, **34**(9), e4876, DOI: 10.1002/bmc.4876.

56 N. Manousi, W. Wojnowski, J. Płotka-Wasylka and V. Samanidou, Blue applicability grade index (BAGI) and software: a new tool for the evaluation of method practicality, *Green Chem.*, 2023, **25**(19), 7598–7604, DOI: 10.1039/D3GC02347H.